

Azide Assisted Corrosion Inhibition of Mild Steel by Bioactive Metallic Complexes - A Quantum Chemical Investigation

Das, Mriganka

Environment Research Group, Research and Development Department, Tata Steel Ltd

Rudra Manish Desai

School of Science, GSFC University

Biswas, Amrita

Department of Chemistry, Manipal University Jaipur

<https://doi.org/10.5109/7183319>

出版情報 : Evergreen. 11 (2), pp.624-631, 2024-06. 九州大学グリーンテクノロジー研究教育センター
バージョン :

権利関係 : Creative Commons Attribution 4.0 International



Azide Assisted Corrosion Inhibition of Mild Steel by Bioactive Metallic Complexes – A Quantum Chemical Investigation

Mriganka Das^{1*}, Rudra Manish Desai², Amrita Biswas^{3*}

¹Environment Research Group, Research and Development Department, Tata Steel Ltd, Jamshedpur, Jharkhand, 831001, India

²School of Science, GSFC University, Vadodara, Gujarat, 391750, India

³Department of Chemistry, Manipal University Jaipur, Jaipur, Rajasthan 303007, India

*Author to whom correspondence should be addressed:

E-mail: amrita.biswas.chem@gmail.com; mrigankachem24@gmail.com

(Received August 12, 2023; Revised April 19, 2024; Accepted April 21, 2024).

Abstract: Corrosion of mild steel is a significant issue in various industrial applications, and the development of effective corrosion inhibitors is crucial for mitigating this problem. In recent years, bioactive metallic complexes have emerged as promising candidates for corrosion inhibition due to their unique properties and environmentally friendly nature. Aiming of this article to study the activity and effectiveness of corrosion inhibitors. Generally, inhibitors work on surface adsorption properties. Here, we are focusing on the study of inhibitor adsorption activity on metal surfaces by theoretical approach. Schiff base compounds show very good interaction with metal surfaces. Inhibitor interaction was measured by the Density Functional Theory study with the help of Gaussian9 and Accelrys Material Studio 7.0. From the calculation of HOMO, LUMO, ΔE , ΔN and Fukui function of Schiff base complex clearly show that the complex 2 has better interaction with metal surface and show maximum efficiency. Very short time of theoretical calculation evidently tells us about the inhibitor activity of Schiff base complex.

Keywords: DFT; Schiff base; Corrosion Inhibitor.

1. Prerequisites for the publication

Corrosion is the severe attack on metals by their environment. Metal corrosion is one of the many issues in chemistry that have been tackled by the engineers and chemists in various industries. Microbial corrosion refers to the impact of different microorganisms on metal. As a result, corrosion inhibition is a tough problem for both chemists and engineers to master¹. Corrosion inhibition by different materials occurs at the surface, where organic as well as inorganic complexes adhere to the metallic surface². The mixture of organic-inorganic hybrid molecules that are quickly active and have efficient surface chemistry to prevent corrosion are quite exciting to consider³. Better understanding the inhibitor's mechanism, it's very important to study the molecular orientation, favorable configuration, steric and electronic impacts, ionic charge on the molecule^{1,4}.

Experiments are typically expensive and complex, but they can be extremely essential in illuminating the inhibition process between metal and inhibitors. The improvement of software as well as hardware has made computational chemistry a valuable tool for corrosion

inhibition research. To link the inhibitors' inhibitory efficacy with their molecular characteristics, a variety of quantum chemistry approaches and molecular modelling techniques have been used. In addition to being generally used to explore reaction pathways, quantum chemical calculations have also been found to be an effective computational research tool for investigating metal corrosion inhibition⁵. The effectiveness of inhibitor molecule is related to both its spatial molecular structure and electronic structure, establishing a link between quantum chemical characteristics and inhibition efficiency⁶. Quantum chemical approaches and molecular modelling techniques enable the description of a vast number of molecular characteristics, such as the reactivity, binding capabilities, and shape of a whole inhibitor molecule, as well as molecular fragments and substituents connected to it⁷.

There haven't been many publications in the literature that investigate zinc complexes as active corrosion inhibitors of stainless steel. Recently our group (Das et al.)⁸ reported biologically active zinc (II) Schiff base complexes as corrosion inhibition. In line with this experimental evidence herein theoretical comparative

studies based on the quantum chemical approach are explored. Density functional theory and nucleophilic site prediction are applied as an evidential approach to measure the comparative corrosion inhibition property among the free amines, Schiff bases, and Zn (II) azido Schiff base complexes⁹. With detailed calculation and based on the hard soft acid base (HSAB) principle the experimental data matches perfectly with the theoretical calculations.

2. Experimental

2.1 Sketching of the molecules with geometry optimization:

Chem-Draw professional 16.0 software is used for the sketching of all amines, ligands and complexes. Geometry optimization is used to refine the geometry of their structures to decrease their conformational and torsional energies. Geometry optimization was done by Gaussian09 software and the calculation of Fukui functions of optimized structure completed with the Accelrys Material Studio 7.0 software.

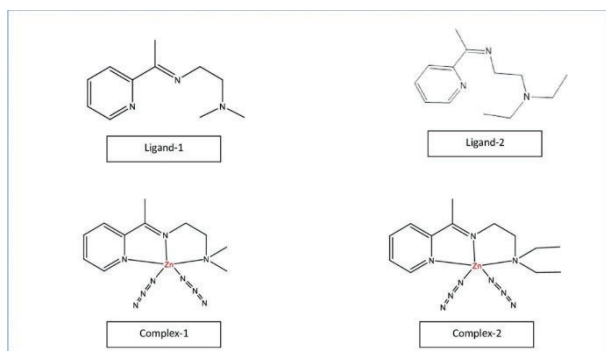


Fig. 1: 2D structures of studied ligands and complexes.

2.2 Quantum Chemical Calculations

The Gaussians 09 package has been used for implementation of RB3LYP level theory for all calculations, which were performed in gaseous phase. For C, N, H, and O, the 6-311G (d, p) basis set is applied, while LANL2DZ is used for Zn in all calculations. The Dmol3 module was utilized to calculate the Fukui functions. The first derivative of the electron density $\rho(r)$ with respect to the number of electrons N , with a constant external potential $v(r)$, is known as the Fukui function (f_k), and it is expressed as follows.

$$f_k = \left(\frac{\partial \rho(\vec{r})}{\partial N} \right)_{v(\vec{r})} \quad (1)$$

To obtain the Fukui function in support of nucleophilic and electrophilic attack, finite difference approximations have been applied,

$$f_k^+ = q_k(N+1) - q_k(N) \quad [\text{For nucleophilic attack}] \quad (2)$$

$$f_k^- = q_k(N) - q_k(N-1) \quad [\text{For electrophilic attack}] \quad (3)$$

Here, q_k stands in for the atom k 's gross charge. The charges of the cationic, neutral, and anionic species are, respectively, denoted $q_k(N-1)$, $q_k(N)$ and $q_k(N+1)$.

3. Results and discussion

3.1 Quantum Chemical Calculations

To investigate the active sites and local reactivity of molecules, quantum calculations were performed using Gaussian09 software. Simulations were also performed for amines, ligands and complexes using density functional theory (DFT) with B3LYP/6-311G basis set in gas phase. To examine the interaction between the frontier orbitals, involving the HOMO and LUMO, the calculations of the frontier molecular orbitals (FMO) have been investigated and simulated¹⁰. The resultant images of FMO with optimized geometry are illustrated in the figure. To minimize the torsional strength, all the molecules are optimized and brought to stable ground state. These calculations explain more about chemical reactivity and selectivity with the help of frontier orbitals (HOMO and LUMO), global hardness (η), global softness (σ), and electronegativity (χ). Furthermore, quantum calculations explain about local reactivity with Fukui function (F_k^+), (F_k^-) and (F_k^0). electron affinity (A) and Ionization potential (I) were computed using the EHOMO and ELUMO, respectively¹¹⁻¹⁴.

$$\chi = \mu = -\left(\frac{\partial E}{\partial N} \right) v(r) \quad (4)$$

μ stands for chemical potential, χ stands for electronegativity, E is total electronic energy and $v(r)$ is external potential.

$$\eta = \left(\frac{\partial^2 E}{\partial N^2} \right) v(r) = \left(\frac{\partial \mu}{\partial N} \right) v(r) \quad (5)$$

η is the second derivative of energy E and is defined as global hardness. It is part of density functional theory (DFT).

$$I = -E_{HOMO} \quad (6)$$

$$A = -E_{LUMO} \quad (7)$$

Here, the energy of the highest occupied molecular orbital (E_{HOMO}) is related to ionization potential (I) and the lowest unoccupied molecular orbital (E_{LUMO}) is related with electron affinity (A).

$$\chi = \frac{I+A}{2} = \frac{E_{LUMO}+E_{HOMO}}{2} \quad (8)$$

$$\sigma = 1/\eta \quad (9)$$

In the following step, Pearson method¹⁵⁾ is used for the calculation of ΔN (fraction of electron transfer) from inhibitor to metal surface by following equation¹⁶⁾.

$$\Delta N = \frac{\chi_{Fe} - \chi_{inh}}{2(\eta_{Fe} + \eta_{inh})}$$

The value of χ_{Fe} is 7 eV and $\eta_{Fe}=0$ eV has been used after referring to available literature to calculate the value of ΔN ^{15,17-21)}.

Table 1: Detailed parameters of theoretical calculation.

Compounds	HO MO (eV)	LU MO (eV)	ΔE (eV)	E_{LUMO} (Fe)- E_{HOMO} (inh) (eV)	χ (eV)	(eV)	ΔN
Complex 1	-5.059	-2.731	2.323	4.935	3.985	1.164	1.334
Complex 2	-5.011	-2.708	2.303	4.887	3.859	1.151	1.364
Ligand-1	-9.022	3.246	12.268	8.898	6.134	2.888	0.149
Ligand-2	-4.818	1.160	3.658	4.694	2.989	1.829	1.096
Amine-1	-5.275	2.244	7.519	5.151	3.759	1.515	1.069
Amine-2	-5.151	2.069	7.222	5.027	3.611	1.541	1.099

The bonding capacity of the molecules were explained by HSAB concept and frontier-controlled interaction^{21,22)}. The electron giving ability is denoted by E_{HOMO} . As a result, high E_{HOMO} values help in the delivery of electrons to an acceptor with a low empty orbital²³⁾. With higher E_{HOMO} levels, the efficiency of inhibition improves. High E_{HOMO} values indicate that the molecule tends to give electrons to the proper acceptor molecules when the molecule possesses a low-energy empty molecular orbital²⁴⁾.

When metal atoms, such as Zn, cohere with hard

molecules, they create a larger HOMO–LUMO gap opposed to when they bind with soft molecules, where a smaller HOMO–LUMO gap is expected¹⁶⁾. The HOMO–LUMO gap of complex 1 is quite larger than complex 2. So, we can conclude that complex 2 is softer than complex 1 from the value obtained in Table 1. The reactivity of the molecules towards the metal surface is evident by the energy gap (ΔE) between HOMO and LUMO¹⁹⁾. The results obtained from (Table 1) indicate that the compound ligand-1 has lowest HOMO energy (E_{HOMO}) whereas the compound ligand-2 has the highest HOMO energy (E_{HOMO}) among these compounds. Also, considering E_{LUMO} , among all other compounds, compound ligand-1 has the highest. It is also evident that ligand-2 has the shortest energy gap ($\Delta E = E_{LUMO(Fe)} - E_{HOMO}$) as compared to other compounds. The smallest energy gap implies that ligand-2 can transfer an electron from HOMO to LUMO level easily. It signifies that this energy gap difference is basically supported by the increase in the LUMO energy of ligand-1 and amine-1 compounds. This implies a decrease in the donor capability. Based on these results, it can be validated that the overlapping of orbitals in ligand-2 is highest in comparison to the rest of the compounds.

Generally, electronegativity values will decrease as inhibition efficiency increase since good inhibitors contribute electrons to the metallic surface²⁵⁾. Additionally, Table 1 shows the values of χ for existing system. The trend in the electronegativity values for the indicated inhibitors shows that ligand-2 has the lowest value. When compared to ligand-1, this action increases its adsorption on the mild steel surface consequently increasing its corrosion prevention performance. Furthermore, to satisfy the study calculation of number of electrons transported (ΔN) were carried out. Pearson method was used to compute the ΔN from the inhibitor to metallic surface. When molecules have a positive ΔN , they are electron donors, and when they have a negative ΔN , they are electron acceptors¹⁶⁾. As per the data in Table 1, ΔN of ligand-1 is the lowest and it indicates that the adsorption of Ligand-1 will be much less as compared to ligand-2. In case of amines, they have similar ΔN . Amine-2 has little more ΔN , which indicates it has higher adsorption tendency than amine 1. For complex 1 and complex 2, the value of ΔN is slightly higher in complex 2 than complex 1. It shows that complex-2 has a better electron transfer system than complex-1, which also justifies the previous experimental conclusion with studied theoretical data. These results justify the chemisorption as well as physisorption which took place for the adsorption of complexes.

Table 2: Concentration dependent EIS data from experimental work⁷⁾.

Inhibitor	Concentration (g/L)	R_s (Ωcm)	$R_p=R_{ct}+R_f$ (Ωcm^2)	N	Y0 ($\mu F/cm^2$)	Cdl ($\mu F/cm^2$)	η_{imp}
-----------	---------------------	-----------------------	------------------------------------	---	---------------------	----------------------	--------------

							(%)
Blank		1.05	17.28	0.8047	405.9	121.79	
Complex-1	0.2	2.63	102.47	0.999	33.20	33.2	83.13
Ligand-1	0.2	1.27	51.94	0.4687	168.10	89.5	66.73
Complex-2	0.2	1.50	135.58	0.999	17.63	17.6	87.25
Ligand-2	0.2	1.27	64.93	0.999	43.69	43.7	73.8

For simplification nomenclature, Complex 3⁷⁾ \equiv Complex 1; Complex 4⁷⁾ \equiv Complex 2.

3.2 Fukui Function

For the additional support, Fukui function calculations were performed, which is a crucial method for identifying the molecular constituents most frequently involved in this donor-acceptor type of interaction²⁶⁾. The local reactivity of a molecule as well as its nucleophilic and electrophilic behavior can be precisely predicted using Fukui indices analysis²⁷⁾. The greater value of f_k^+ denotes the metal surface's acceptance of an electron, while the larger value of f_k^- signifies the inhibitor molecules' greater potential for electron donation¹⁶⁾.

Table 3: Fukui functions for complex

COMPLEX 1				COMPLEX 2			
Atoms	f_k^+	Atoms	f_k^+	Atoms	f_k^+	Atoms	f_k^+
Zn(1)	-0.012		0.004	Zn(1)	-0.006		0.006
	0.055		0.015		0.014		0.003
N(2)	0.093		0.025		0.075		0.041
	-0.013		0.014		0.036		0.009
N(4)	-0.038		0.059		0.024		0.017
	0.012		0.034		0.046		0.004
N(6)	0.06		0.125		0.091		0.012
	0.019						

N(8)	0.003	0.152	0.077	C(8)	-0.024	-0.006	-0.015
	0.004	0.062	0.032	C(9)	-0.047	0.007	0.023
N(10)	0.055	0.192	0.123	C(10)	-0.017	0.007	0.008
	0.011	0.009	0.001	C(11)	0.011	0.002	0.006
H(12)	0.053	0.001	0.026	C(12)	0.007	0.009	0.008
	0.073	0.006	0.043	C(13)	0.003	0.004	0.003
H(14)	0.066	0.025	0.046	C(14)	0.006	0.008	0.007
C(15)	0.036	0.013	0.023	N(15)	0.057	-0.033	0.013
	0.064	0.037	0.047	N(16)	0.098	0.026	0.036
C(17)	0.021	0.009	0.015	N(17)	0.007	0.012	-0.01
	0.055	0.026	0.044	N(18)	0.032	0.154	0.061
C(19)	0.046	0.004	0.021	N(19)	0.013	0.056	0.034
C(20)	0.087	0.012	0.052	N(20)	0.069	0.189	0.124
	0.024	0.006	0.015	N(21)	0.035	0.169	0.067
H(22)	0.043	0.022	0.032	N(22)	0.014	0.058	0.036
H(23)	0.038	0.013	0.026	N(23)	0.063	0.195	0.129
	0.043	0.014	0.029	H(24)	0.053	0.001	0.026
C(25)	0.038	0.009	0.024	H(25)	0.066	0.023	0.044
H(26)	0.054	0.027	0.037	H(26)	0.063	0.028	0.045
H(27)	0.044	0.021	0.033	H(27)	0.054	0.024	0.039
C(28)	-0.01	-0.01	0.01	H(28)	0.044	0.013	0.028

	1		1				
H(29)	0.016	-0.005	0.005	H(29)	0.045	0.015	0.027
H(30)	0.037	0.035	0.036	H(30)	0.044	0.018	0.031
C(31)	-0.005	-0.007	-0.006	H(31)	0.043	0.021	0.032
H(32)	0.027	0.036	0.031	H(32)	0.052	0.016	0.034
H(33)	0.013	-0.016	0.001	H(33)	0.035	0.03	0.033
H(34)	-0.013	0.015	0.001	H(34)	0.013	-0.01	0.002
C(36)	-0.011		-0.006	H(35)	0.003	-0.015	-0.006
H(37)	0.026	0.038	0.032	H(36)	0.023	0.035	0.029
H(38)	0.009	-0.003	0.003	H(37)	-0.004	-0.033	-0.018
H(39)	0.011	0.011	0	H(38)	0.022	0.031	0.026
				H(39)	0.009	0.013	0.011
				H(40)	-0.017	0.011	-0.003
				H(41)		-0.021	-0.005
				H(42)	0.001	0.019	0.01
				H(43)	0.019	0.019	0.019
				H(44)	0.018	0.012	0.015

Table 4: Fukui functions for ligand

LIGAND 1				LIGAND 2			
Atoms	Fk+	Fk-	Fk0	Atoms	Fk+	Fk-	Fk0
N(1)	0.087	0.004	0.046	C(1)	0.011	0.004	0.008
N(2)	0.096	0.011	0.043	C(2)	0.083	0.013	0.048
N(3)	-0.028	0.25	0.111	C(3)	0.057	0.007	0.028
C(4)	0.00	0.00	0.00	C(4)	0.01	0.00	0.01

	9	5	7		3	7	
H(5)	0.072	0.023	0.048	C(5)	0.065	-0.005	0.03
C(6)	0.092	0.012	0.051	C(6)	0.053	0.014	0.034
H(7)	0.082	0.027	0.055	C(7)	-0.025	0.011	-0.018
C(8)	0.057	0.005	0.031	C(8)	-0.037	-0.02	-0.028
H(9)	0.077	0.021	0.049	C(9)	-0.014	0.056	-0.035
C(10)	0.006	0.005	0	C(10)	0.002	0.062	0.032
H(11)	0.066	0.008	0.029	C(11)	-0.004	0.036	-0.02
C(12)	0.077	0.005	0.036	C(12)	-0.012	0.052	0.032
C(13)	0.041	0.001	0.021	C(13)	0.008	0.021	0.014
C(14)	-0.024		0.012	N(14)	0.082	-0.024	0.029
H(15)	0.054	0.036	0.009	N(15)		-0.031	0.04
H(16)	0.026	0.041	0.033	N(16)	-0.007	0.254	0.124
H(17)	0.048	0.03	0.039	H(17)	0.068	0.013	0.04
C(18)	-0.028	-0.022	-0.025	H(18)	0.079	0.027	0.053
H(19)	0.037	0.029	0.033	H(19)	0.073	0.026	0.049
H(20)	0.048	0.062	0.055	H(20)	0.061	0.016	0.039
C(21)	-0.012	-0.056	-0.034	H(21)	0.044	-0.003	0.021
H(22)	0.017	0.068	0.043	H(22)	0.047	0.033	0.04
H(23)	0.043	0.105	0.074	H(23)	0.032	0.024	0.028
C(24)	-0.013	-0.068	-0.041	H(24)	0.056	0.058	0.057
H(25)	0.03	0.12	0.07	H(25)	0.04	0.03	0.03

)		8	9)	1	1	6
H(26)	0.01	0.08	0.04	H(26)	0.03	0.06	0.05
)	6	2	9)	7	6	2
H(27)	0.00	0.08	0.04	H(27)		0.09	0.05
)	2	2	2)	0.02	7	8
C(28)	-	-	-	H(28)	-	0.03	0.06
)	7	3	5)	4	2	4
H(29)		0.13	0.08	H(29)	0.02	0.10	0.06
)	0.03	2	1)	8	9	9
H(30)	-			H(30)	-		
)	0.01	0.08	0.03)	0.01	0.04	0.01
H(31)	2	3	6)	1	3	6
)	0.01	0.08	0.04	H(31)	0.00	0.06	0.03
	4	3	8)	6	6	6
				H(32)			0.03
)	0.03	0.04	5
				H(33)	0.01	0.07	0.04
)	3	5	4
				H(34)	0.01		0.04
)	5	0.07	3
				H(35)	0.00	0.04	0.02
)	6	6	6
				H(36)	0.02	0.07	0.05
)	4	9	1
				H(37)	0.00		0.02
)	7	0.04	4

Table 3 and Table 4 represent the calculated Fukui indices. The outcomes of the calculations show that the azide and acetyl pyridine moiety's N and C atoms are the most open to accepting or donating electrons. For complex 2, relatively high f_k^- values was noticed for atoms like

Fig. 2: The frontier molecular orbital figures of studied molecules.

N(18), N(20), N(21), N(22) and N(23) which indicate that N atoms of azide has higher affinity to donate electrons to the steel surface. Ligand-2 has lower f_k^- values in compared to complex-2, which suggest that the greater number of N will help to donate more electrons and it will have higher affinity towards steel surface¹⁶. In complex 1, value of f_k^+ of the following atoms: N(2), N(3), C(13) and C(20) prove that the pyridine ring's C atoms and the terminal N atoms of azide are take electron from the mild steel surface. The value from the table clearly proves that Zn(1) in Complex 1 is less likely than complex 2 to absorb electrons from the surface of steel. Similarly, While the N atoms in the azide component of complex 2 are more capable of donating electrons, the C atoms on the acetyl pyridine ring encourage higher acceptance of electrons from metallic surfaces. Complex 2 is better at preventing efficiency than complex 1 because it has more heteroatoms than complex 1, which gives that compound a susceptibility for both electrophilic and nucleophilic approach.

3.3 Molecular electrostatic potential surface (MEP):

Over the last 30 years, molecular electrostatic potential (MEP) has been used widely in scientific research for the investigation. Reactivity of molecules towards charged species can be determine by electrical potential²⁸. Sensitivity of molecules with nucleophilic and electrophilic reactants can be determine with the MEP. To get shape, size and charge all at once; Molecular electrostatic potential surfaces are reliable tools for it²⁹.

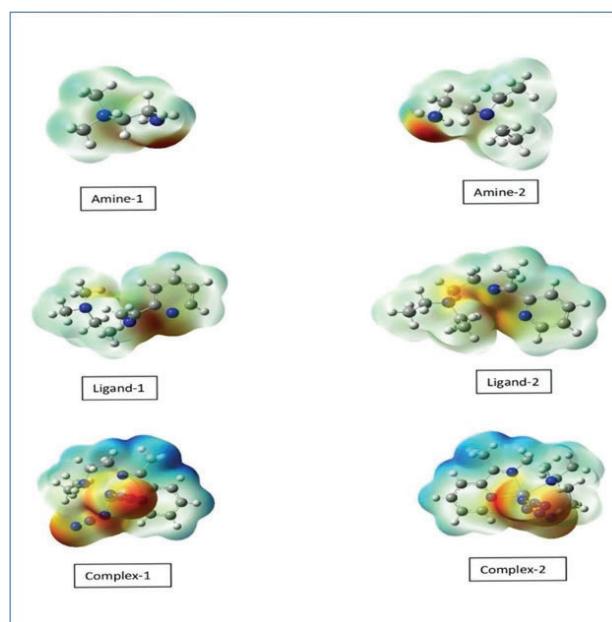
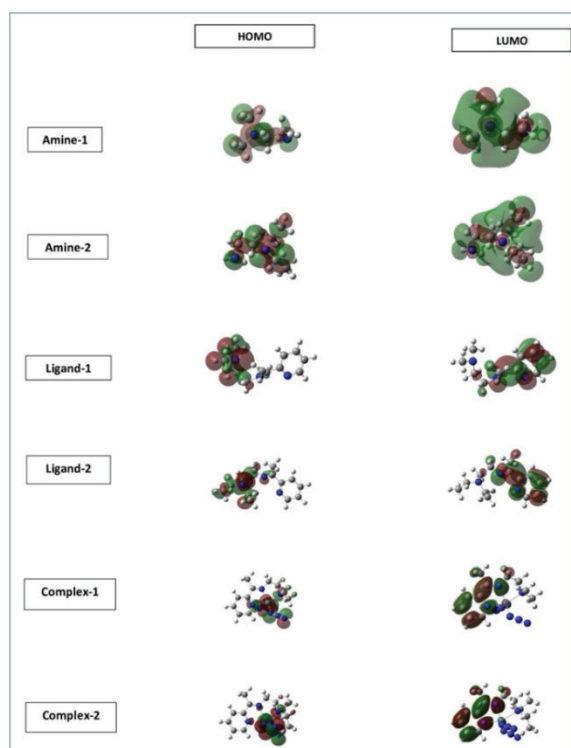


Fig. 3: Molecular electrostatic potential surfaces of the studied molecules

For analysis, geometry optimization was done by DFT

method at B3LYP level of approximation with 6-311+G (d, p) basis set to determine the features of amines, ligands and metal complexes. Accelrys Material Studio 7.0 software is used for visualization purposes as shown in Fig. 3. The magnitude of electrostatic potential can be determined by the several different colors of MEP surfaces. Red represents the highest potential followed by orange, yellow, green and blue. Blue color represents the least magnitude of electrostatic potential in the molecule¹¹⁾. Red regions are more suitable regions for the electrophilic attack because of red color infers as negative potential and electron rich regions. Usually, over hydrogen atoms and carbon atoms have blue and green color regions, which indicates positive potential and it favors nucleophilic attack²⁹⁻³¹⁾.

4. Conclusion

The theoretical study of pseudo-halide promoted corrosion inhibitors were successfully performed using DFT with B3LYP/6-311G and quantum chemical parameters connected to the inhibitor molecules' electronic structures confirmed their ability to inhibit through HOMO, LUMO, ΔN , electron densities, while Fukui indices suggest that the molecules may adsorb to the surface of steel through free sites of N atoms in complex. The presence of free N enhances the ability of inhibition. The comparative study of ligands and complexes gives the important conclusion that complexes are better inhibitors because of the free N atoms. A similar pattern was also followed in the experimental study of the inhibitors which proves the credibility of the theoretical data.

Acknowledgements

The authors are grateful for the support from IIT Indore, Tata Steel R&D, Manipal University Jaipur and GSFC University for successful completion of this project. The authors did not receive any funding from any organization for conducting this study.

References

- 1) R. Zulkafli, N. K. Othman*, N. Yaakob, F. K. Sahrani, M.S.H Al-Furjan, "Electrochemical Studies of Microbiologically Influenced Corrosion on API 5L X65 by Sulfate-Reducing Bacteria in CO₂ Environments," *Evergreen*. 10 601–607 (2023). <https://doi.org/10.5109/6782167>
- 2) A.S. Idris, S. Ghosh, H. Jiang, and K. Hamamoto, "A multi-layer stacked all sol-gel fabrication technique for vertical coupled waveguide," *Evergreen*. 4 (2/3) 12–17 (2017). doi:10.5109/1929657
- 3) A. Trentin, T.A.C. de Souza, M.C. Uvida, "Organic-Inorganic Hybrid Coatings for Active and Passive Corrosion Protection, in: S. v Harb (Ed.)," *Corrosion*, IntechOpen, Rijeka, 2020. <https://doi.org/10.5772/intechopen.91464>.
- 4) F. Yulia, S. Marsya, Y. Bobby, Nasruddin, and A. Zulys, "Design and preparation of succinic acidbased metal-organic frameworks for CO₂ adsorption technology," *Evergreen*. 7 (4) 549–554 (2020). doi:10.5109/4150475.
- 5) E.E. Ebenso, T. Arslan, F. Kandemirli, N. Caner, I. Love, "Quantum chemical studies of some rhodanine azosulpha drugs as corrosion inhibitors for mild steel in acidic medium," *Int J Quantum Chem*. 110 1003–1018 (2010). <https://doi.org/https://doi.org/10.1002/qua.22249>.
- 6) P. Udhayakala, T.V. Rajendiran, S. Gunasekaran, "Theoretical Evaluation of Corrosion Inhibition Performance of Some Triazole Derivatives," *J Adv Scient Res*. 3(2) 71–77 (2012). <http://www.sciensage.info/jasr>
- 7) A. Kumar, A.K. Chanda, and S. Angra, "Numerical modelling of a composite sandwich structure having non metallic honeycomb core," *Evergreen*. 8 (4) 759–767 (2021). doi:10.5109/4742119.
- 8) M. Das, A. Biswas, B. Kumar Kundu, M. Adilia Januário Charmier, A. Mukherjee, S.M. Mobin, G. Udayabhanu, S. Mukhopadhyay, "Enhanced pseudo-halide promoted corrosion inhibition by biologically active zinc(II) Schiff base complexes," *Chem. Eng. J*. 357 447–457 (2019). <https://doi.org/10.1016/j.cej.2018.09.150>.
- 9) H. Ebrahimi, J. Hadi, Z.A. Abdulnabi, Z. Bolandnazar, "Spectroscopic, thermal analysis and DFT computational studies of salen-type Schiff base complexes," *Spectrochim Acta A Mol Biomol Spectrosc*. 117 485–492 (2014). <https://doi.org/10.1016/j.saa.2013.08.044>.
- 10) M. Shahraki, M. Dehdab, S. Elmi, "Theoretical studies on the corrosion inhibition performance of three amine derivatives on carbon steel: Molecular dynamics simulation and density functional theory approaches," *J Taiwan Inst Chem Eng*. 62 313–321 (2016). <https://doi.org/10.1016/j.jtice.2016.02.010>.
- 11) C.D. D Sundari, S. Setiadji, M.A. Ramdhani, A.L. Ivansyah, N.I. T Widhiasiari, "Additional Halogen Group (F, Cl, and Br) to 2-Phenyl-imidazole[1,2a]pyridine on Corrosion Inhibition Properties: A Computational Study," *IOP Conf Ser Mater Sci Eng*. 288 012033 (2018). <https://doi.org/10.1088/1757-899X/288/1/012033>.
- 12) I.A.A. Aziz, I.A. Annon, M.H. Abdulkareem, M.M. Hanoon, M.H. Alkaabi, L.M. Shaker, A.A. Alamiery, W.N.R. Wan Isahak, M.S. Takriff, "Insights into Corrosion Inhibition Behavior of a 5-Mercapto-1, 2, 4-triazole Derivative for Mild Steel in Hydrochloric Acid Solution: Experimental and DFT Studies," *Lubricants*, 9 122 (2021). <https://doi.org/10.3390/LUBRICANTS9120122>.
- 13) N.O. Eddy, P.O. Ameh, N.B. Essien, "Experimental and computational chemistry studies on the inhibition

- of aluminium and mild steel in 0.1 M HCl by 3-nitrobenzoic acid," *J. Taibah Univ. Sci.* 12 545–556 (2018).
<https://doi.org/10.1080/16583655.2018.1500514>.
- 14) J. F. Fatriansyah*, S. R. Kurnianto, S. N. Surip, A. F. Pradana, A. G. Boanerges, "Molecular Docking and Molecular Dynamics of Herbal Plants *Phyllanthus Niruri* Linn (Green Meniran) towards of SARS-CoV-2 Main Protease," *Evergreen*. 10 731–741 (2023).
<https://doi.org/10.5109/6792822>
 - 15) S. Martinez, "Inhibitory mechanism of mimosa tannin using molecular modeling and substitutional adsorption isotherms," *Mater Chem Phys.* 77 97–102 (2003).
[https://doi.org/10.1016/S02540584\(01\)00569-7](https://doi.org/10.1016/S02540584(01)00569-7).
 - 16) M. Das, A. Biswas, B.K. Kundu, S.M. Mobin, G. Udayabhanu, S. Mukhopadhyay, "Targeted synthesis of cadmium(II) Schiff base complexes towards corrosion inhibition on mild steel," *RSC Adv.* 7 48569–48585 (2017).
<https://doi.org/10.1039/c7ra08633d>.
 - 17) A. Aouniti, H. Elmsellem, S. Tighadouini, M. el Azzouzi, S. Radi, A. Chetouani, B. Hammouti, A. Zarrouk, "Schiff's base derived from 2-acetyl thiophene as corrosion inhibitor of steel in acidic medium," *J. Taibah Univ. Sci.* 10 774–785 (2016).
<https://doi.org/10.1016/j.jtusci.2015.11.008>
 - 18) K. Ragi, J.T. Kakkassery, V.P. Raphael, B.M. Paulson, R. Johnson, "Corrosion inhibition of mild steel by N, N'-(5,5-dimethylcyclohexane-1,3-diylidene)dianiline in acid media: Gravimetric and electrochemical evaluations," *Curr. Chem. Lett.* 10 67–80 (2021).
<https://doi.org/10.5267/j.ccl.2020.8.001>.
 - 19) S. Kaya, P. Banerjee, S.Kr. Saha, B. Tüzün, C. Kaya, "Theoretical evaluation of some benzotriazole and phosphono derivatives as aluminum corrosion inhibitors: DFT and molecular dynamics simulation approaches," *RSC Adv.* 6 74550–74559 (2016).
<https://doi.org/10.1039/C6RA14548E>.
 - 20) H. Rahmani, K. Ismaili Alaoui, K.M. Emran,* A. E. Hallaoui, M. Taleb, S. E. Hajji, B. Labriti, E. Ech-chihbi, B. Hammouti, "Experimental and DFT Investigation on the Corrosion Inhibition of Mild Steel by 1, 2, 3- triazole Regioisomers in 1M hydrochloric Acid Solution," *Int. J. Electrochem. Sci.* 14 985–998 (2014). doi:10.20964/2019.01.80
 - 21) E.C. Koch, "Acid-base interactions in energetic materials: I. The Hard and Soft Acids and Bases (HSAB) principle - Insights to reactivity and sensitivity of energetic materials," *Propellants, Explosives, Pyrotechnics*, 30 5–16 (2005).
<https://doi.org/10.1002/prep.200400080>.
 - 22) R.G. Pearson, "Absolute electronegativity and hardness: application to inorganic chemistry," *Inorg Chem.* 27 734–740 (1988).
<https://doi.org/10.1021/ic00277a030>.
 - 23) A.A. Alamiery, "Case Study in a Conceptual DFT Investigation of New Corrosion Inhibitor," *Lett. Appl. NanoBioScience.* 11 4007–4015 (2021).
<https://doi.org/10.33263/lianbs114.40074015>.
 - 24) S.K. Saha and P. Banerjee, "A theoretical approach to understand the inhibition mechanism of steel corrosion with two aminobenzonitrile inhibitors," *RSC Adv.* 5 71120–71130 (2015).
<https://doi.org/10.1039/C5RA15173B>.
 - 25) B.A. Umar and A. Uzairu, "In-silico approach to understand the inhibition of corrosion by some potent triazole derivatives of pyrimidine for steel," *SN Appl Sci.* 1 1413 (2019). <https://doi.org/10.1007/s42452-019-1451-y>.
 - 26) K.M. Merz and J. Faver, "Utility of the hard/soft acid-base principle via the fukui function in biological systems," *J Chem Theory Comput.* 6 548–559 (2010).
<https://doi.org/10.1021/ct9005085>.
 - 27) Y. Li and J.N.S. Evans, "The Fukui Function: A Key Concept Linking Frontier Molecular Orbital Theory and the Hard-Soft-Acid-Base Principle," (1995).
 - 28) J.M. Campanario, E. Bronchalo, M.A. Hidalgo, "An Effective Approach for Teaching Intermolecular Interactions," (1994).
 - 29) F.J. Luque, J.M. López, M. Orozco, Perspective on "Electrostatic interactions of a solute with a continuum. A direct utilization of ab initio molecular potentials for the prevision of solvent effects," *Theor Chem Acc.* 103 343–345 (2000).
<https://doi.org/10.1007/s002149900013>.
 - 30) S.H. Sumrra, W. Zafar, M.L. Asghar, F. Mushtaq, M.A. Raza, M.F. Nazar, M.A. Nadeem, M. Imran, S. Mumtaz, "Computational investigation of molecular structures, spectroscopic properties, cholinesterase inhibition and antibacterial activities of triazole Schiff bases endowed metal chelates," *J Mol Struct.* 1238 130382–130394 (2021).
<https://doi.org/10.1016/j.molstruc.2021.130382>.
 - 31) R. Joshi, A. Kumari, K. Singh, H. Mishra, S. Pokharia, "Triorganotin(IV) complexes of Schiff base derived from 1,2,4-triazole moiety: Synthesis, spectroscopic investigation, DFT studies, antifungal activity and molecular docking studies," *J Mol Struct.* 1206 127639–127653 (2020).
<https://doi.org/10.1016/j.molstruc.2019.127639>.